International Journal for Ion Mobility Spectrometry (2020) 23:133–142
https://doi.org/10.1007/s12127-020-00261-4

ORIGINAL RESEARCH

Enabling resolution of isomeric peptides using tri-state ion gating and Fourier-transform ion mobility spectrometry

Pearl Kwantwi-Barima[1] · Tobias Reinecke[1] · Brian H. Clowers[1]

Received: 8 April 2020 / Revised: 8 April 2020 / Accepted: 13 May 2020 / Published online: 28 May 2020

Abstract

Using Fourier-Transform ion gate modulation technique, we compare the ability of the tri-state ion shutter (3S-IS) to the two-state ion shutter (2S-IS) in separating three pairs of isomeric peptide including 1.Gly-Arg-Gly-Asp-Ser (GRGDS) / Ser-Asp-Gly-Arg-Gly (SDGRG); 2.Sar-Arg-Gly-Asp-Ser-Pro (SRGDSP) / Gly-Arg-Gly-Asp-Thr-Pro (GRGTP); 3.Kemptide / (Val^6, Ala^7)-Kemptide using electrospray ionization and ion mobility spectrometry. Mobility separation was evaluated for peptide individually and as simple mixtures. Baseline resolution of both singly and doubly charged ions of the isomeric pentapeptide mixture of GRGDS / SDGRG was attainable with the described IMS system using the 3S-IS configuration, illustrating the capacity of the present instrument to resolve isomeric compounds with differences in ion neutral collision cross section (CCS) of less than 1% for the singly charged ions. However, with the 2S-IS, both singly and doubly charged ions of the same peptide mixture were unresolved in the mobility domain. To our knowledge, this is the first-time baseline separation has been reported for the singly charged ions of the isomeric reversed sequence pentapeptide mixture using Fourier transformed drift tube IMS with nitrogen as the drift gas. For all the peptide mixtures, the ion counts for the ion mixture recorded with the 3S-IS were substantially higher (> 50%) in comparison to the 2S-IS. The resolving power of the instrument ranged between 82 to 128 for the target analyte ions analyzed in a mixture using the 3S-IS. Whereas, the resolving power of the 2S-IS ranged between 60 and 100 for the target analytes. Overall, a 20% increase in resolving power was obtained with the 3S-IS in comparison to the 2S-IS. Separation of the different isomeric peptide ion mixture depicted in this present study clearly shows the unique size-to-charge separation ability of IMS that complements the mass-to-charge ratio measurement capacity of mass spectrometry.

Keywords Ion mobility spectrometry · Electrospray, Fourier-transform ion mobility spectrometry · Tri-state ion shutter

Introduction

The physiological properties of proteins, peptides, high-molecular weight compounds and other biologically active compounds are strongly related to their structures. Hence, structure determination of the aforementioned compounds are pertinent. Mass spectrometry (MS) based analytical techniques have widely been used to analyze and characterize peptides,[1, 2] proteins,[3, 4][1, 5], [3, 4],[1, 5] and other types of molecules including isotopes[6–8]and isotopologues[9–11] with high sensitivity. However, as a technique which measures the mass-to-charge ratio of ions, MS suffers from the inability to separate gaseous isomers and conformers.[12–14] Ion mobility spectrometry (IMS) finds growing utility in efforts to probe the shape and conformation of small molecules and proteins in the gas-phase by separating ions based on their gas-phase ion mobilities which is conceptually linked to the concept of a charge-normalized collision cross section.[15, 16] When combined with mass spectrometry, IM-MS offers a tractable path to achieve isomeric separations by providing structural information of molecules of interest since the structural separation obtained by IMS is uniquely different from mass-to-charge information. The application of IM-MS as analytical technique has evolved to include a broad range of research disciplines from structural biology analysis,[17] drug metabolism,[18] native protein-protein assemblies,[19] isomeric separations,[20–22] and molecular class differentiation.[23, 24].

Despite the broad applicability and increasing usage, ion mobility is a relatively low resolution separation technique. Signal average measurements made with traditional drift tube

✉ Brian H. Clowers
brian.clowers@wsu.edu

[1] Department of Chemistry, Washington State University, Pullman, WA 99164, USA

systems suffer from poor sensitivity due to its inherent low duty cycle related to the period between ion gating cycles and the initial width of the ion packets injected into the drift tubes. Multiplexing techniques based on ion-gate modulation, such as Hadamard and Fourier-transform, are known to provide a solution to the low duty cycles observed in signal averaged drift tube systems.[25–27] Fourier-transform based ion gate modulations have made it possible to couple IMS experiments to mass analyzers with lower sampling rates such ion traps,[26, 28, 29] and obitraps,[30] with a 25-fold enhancement in duty cycle compared to signal averaged ion mobility experiments. Some isomeric species require higher resolution in the ion mobility spectrometer to achieve separation.[22] Therefore, for IM-MS techniques that use linear frequency modulation as a mobility encoding scheme, higher resolution separations are accessed through efficient ion gating and higher frequencies.[28] However, ion gate depletion effects (widely described in Bradbury-Neilson (BN) ion shutters)[25, 31, 32] are known to severely impact slower moving ions (i.e. lower mobilities) and are exacerbated at higher ion gating frequencies.[21] Regardless of the ion transmission mechanisms used in either high pressure or low pressure drift tube IMS experiments, mobility bias exists. For low-pressure drift tube IMS systems using ion funnel traps as the means of ion injection, efforts to reduce ion discrimination by employing helium as a trapping gas have shown promise, however, this work conducted by Ibrahim et al. requires a careful balance of differential pressures and is not applicable to drift tube IMS systems with pressures much above 10 Torr.[33].

Recently, Kirk et al. described an improved configuration (known as tri-state, tri-grid ion shutter (3S-IS)) [34] based upon the previous tri-grid ion shutter (two-state ion shutter (2S-IS))[35] which showed a significant improvement over the signal averaged mode experiments with a major decrease in ion depletion effect for a gate pulse width of 1 μs.[34] In our recent publication,[21] a comparison of the performance levels of the 3S-IS to 2S-IS were made for a series of Fourier-transform ion mobility mass spectrometry experiments. The 3S-IS and 2S-IS comparison were made using compounds with a range of reduced mobilities such as peptides and a series of tetraalkylammonium salts (T5-T8, T10 and T12 ions). Increases in ion counts of 95% and 45% for T5 and T12 ions respectively were reported with the 3S-IS compared to the 2S-IS. Overall a 10% increase in resolving power was achieved with the 3S-IS compared to the 2S-IS. Furthermore, from the same publication, we were able to perform isomeric separation for two reversed sequence pentapeptides using the 3S-IS. With a resolving power of 79 and 57 reported for SDGRG and GRGDS singly charged ions using 3S-IS, a clear discrimination between the two isomers were observed although a baseline resolution was not achieved for these two singly charged species.

Building upon the isomeric separation experiments made in our previous publication, the purpose of this present study is to perform ion mobility separations on different pairs of isomeric species using ion mobility coupled to a linear ion trap mass spectrometer with a Fourier-based ion gate modulation technique in combination with the 3S-IS and 2S-IS. A comparison of the ion mobility separations achieved using the 3S-IS and 2S-IS was investigated for a mixture of reversed sequence pentapeptides, hexapeptides, and heptapeptides.

Experimental

Chemicals and Reagents. The target analytes chosen were different pairs of isomeric peptides. These included: (1) Gly-Arg-Gly-Asp-Ser (GRGDS)/Ser-Asp-Gly-Arg-Gly (SDGRG);[21] (2) Sar-Arg-Gly-Asp-Ser-Pro (SRGDSP)/ Gly-Arg-Gly-Asp-Thr-Pro (GRGTP);[22] (3) Leu-Arg-Arg-Ala-Ser-Leu-Gly (Kemptide)/Leu-Arg-Arg-Ala-Ser-Val-Ala (Val^6, Ala^7-Kemptide).[22] In addition to the analytes listed above, HPLC grade methanol,water and 0.1% formic acid (ACS reagent grade, >=97 or 98% purity) were purchased from Sigma Aldrich Chemical Co. (Milwaukee, WI, USA). These mixtures were infused into a custom electrospray ionization emitter consisting of a 75 μm glass capillary with the terminating polyimide coating removed. Each isomeric peptide pair was formulated at a concentration of 50 μM in 80/20 HPLC grade methanol / water with 0.1% formic acid respectively.

Atmospheric dual-gate Ion Mobility-Mass Spectrometry. The drift time measurements were made using an atmospheric pressure, PCB-dual ion shutter ion mobility spectrometer coupled to a linear ion trap mass spectrometer. The PCB-dual ion shutter IMS were modelled after the design described by Reinecke and Clowers.[36] The aforementioned dual ion shutter IMS was sealed by using teflon spacers tightly compressed between the electrodes used for both the desolvation region (10.02 cm) and the drift tube. The length of the drift tube was approximately 18.5 cm (with a length of 17.5 cm between the first and second gate). The mass-selected mobility spectra were obtained using the PCB-IMS coupled to a linear ion trap mass spectrometer,(LTQ-XL, Thermo Fisher Scientific, Thousand Oaks, CA) by frequency encoding the mobility data.[21] With the linear ion trap mass spectrometer as the detector, the ion trap was filled for a fixed amount of time by setting the target accumulation population to a large value as AGC could not be turned off in the standard LTQ-XL control software. With this known AGC setting in place, a maximum injection time of 100 ms and *m/z* ranges 50–500, 50–700, and 50–800 were used for the analysis of reversed sequence pentapeptide, hexapeptide, and heptapeptide respectively. The frequency modulated IMS experiments (Fourier Transform-IMS (FT-IMS)) were swept from 5 to 10,005 Hz

over the course of 8 min. In addition to the experimental conditions listed above, the analytes were electrosprayed at a flow rate of 3 μL/min through a 75 μm glass capillary. An electrospray ionization voltage of 2500 V (relative to the first IMS electrode) was used. With the potential of the first IMS electrode held at 15000 V, an electric field of ~467 V cm^{-1} was realized. The IMS was operated at atmospheric pressure (~ 690 Torr in Pullman WA) and maintained at room temperature (23 °C). A countercurrent nitrogen gas flow of 2.5 L/min was allowed into the drift tube (This higher value of drift gas flow was used to account for the API inlet for the mass analyzer). The ions were gated using the two-state, tri-grid ion shutter (2S-IS)[35] and the tri-state, tri-grid ion shutter (3S-IS) principles with the latter first being introduced by Kirk et al.[34] and also described in great detail in our recent publication.[21] The first and second gate were operated with open source ion gate pulsers [37] triggered using a National Instruments Multifunctional DAQ (USB-6531, National Instruments, Austin, TX) that provided the waveforms needed for the experiments. The linearly swept waveforms were delivered to the ion gating electronics through the USB-6531 by leveraging the built-in tools found in the NIDAQ Tools module extension for IGOR Pro (Lake Oswego, OR). We note that a potential of 150 V was applied to completely close the gate in order to stop ions from entering the drift region. Structurally, the arrangement and assembly of the gates are in the same order as that reported by Kwantwi-Barima et al.[21].

Discussion

For all the peptides analyzed, both singly and doubly charged ions were observed in our FT-IMMS experiments. The reduced mobility (K_0) and ion-neutral collision cross section (CCS) for each peptide ion reported in Table 1 were calculated from the individual analyte measurements and not the peptide mixture. Figure 1 is the mass selected mobility spectra for reversed sequence pentapeptide GRGDS and SDGRG obtained through FT-IMMS experiment from 5 to 10,005 Hz for 8 min. Figure 1a and b represent the singly and doubly protonated ions of isomeric pentapeptide mixture using the 2S-IS and 3S-IS respectively. Whereas, Fig. 1c depicts the singly and doubly charged ions of the individual pentapeptide target analytes. For the 3S-IS, baseline separation was achieved for both singly and doubly protonated ions of the isomeric pentapeptide mixture. However, for the 2S-IS, both singly and doubly charged ions of the pentapeptide mixture remained unresolved in the mobility domain as depicted in Fig. 1a. The separation of the singly and doubly protonated ions were due to the small differences in their conformational structure measurable as ion-neutral collision cross section (CCS). The CCS values calculated from the experimental measurements were 205 ± 0.42 $Å^2$, 203 ± 0.43 $Å^2$, 269 ± 0.89 $Å^2$, 274 ± 0.87 $Å^2$ for $[GRGDS+H]^+$, $[SDGRG+H]^+$, $[GRGDS+2H]^{2+}$, and $[SDGRG+2H]^{2+}$ respectively. The original measurements of GRGDS and SDGRG by Wu et al. were conducted using a high temperature drift cell with subsequent measurements made independently by Bush et al.[38], and May et al.[24] Recognizing that the conditions used by May et al. [24] are most similar to the present instrument (i.e. room temperature, nitrogen gas) the singly charged values (205.9 ± 0.2 $Å^2$, 204.6 ± 0.5 $Å^2$ for $[GRGDS+H]^+$ and $[SDGRG+H]^+$ respectively) agree within experimental error of 0.5%. Unfortunately, in that effort, data for the double charged species were not reported. Close examination of the reported literature for the doubly charged species highlights a gap in the consistency of measurement conditions which hinders direct comparisons. Placing the present values for the doubly charged species in the context of the elevated temperature work of Wu et al.,[22] (222.7 $Å^2$, 211.7 $Å^2$ for $[SDGRG+2H]^{2+}$ and $[GRGDS+2H]^{2+}$ respectively) and the radially confining drift cell by Bush et al.[38] (259 $Å^2$, 256 $Å^2$ for $[SDGRG+2H]^{2+}$ and $[GRGDS+2H]^{2+}$ respectively); which itself slightly elevates the effective temperature of the ion, the trends in our data agree with the notion of effective temperature in a radially confining cell (within an experimental error of 6%), and the non-linear dependence of mobility on temperature from a qualitative perspective. It is for these reasons that the values reported here for the double charged species require continued verification using different experimental systems and nominally the same environmental conditions. Furthermore, from the structure of the peptides, the charge location for the doubly protonated ions can reasonably be predicted from the N-terminal residue and the the basic arginine group (Gly**H**$^+$-Arg**H**$^+$-Gly-Asp-Ser; Ser**H**$^+$-Asp-Gly-Arg**H**$^+$-Gly). From the CCS values listed in Table 1 for the doubly charged ions, the $[SDGRG+2H]^{2+}$ seems to exhibit a more extended conformation where the charges are separated from each other (hence the larger CCS value of 259 $Å^2$) stabilized by surrounding carbonyl groups than the $[GRGDS+2H]^{2+}$ which may exhibit a more compact conformation (smaller CCS value of 256 $Å^2$) due to the location of the charges and hence presumably providing more coulombic repulsion as reported by Wu et al.[22] In Table 2, the ion counts recorded for the isomeric pentapeptide mixture at *m/z* 246 and *m/z* 491 with the 3S-IS were 9.91×10^3 and 2.25×10^4 corresponding to a 93.3% and 84.0% increase for *m/z* 246 and *m/z* 491 respectively in comparison to the 2S-IS. The resolving powers for the reversed sequence pentapeptide mixture with the 3S-IS were 100 and 115 for $[GRGDS+H]^+$, $[SDGRG+H]^+$ respectively and 128, 82 for $[GRGDS+2H]^{2+}$ and $[SDGRG+2H]^{2+}$ respectively. The resolving powers for the individual species were 104 for both $[GRGDS+H]^+$, $[SDGRG+H]^+$ and 49, 50 for $[GRGDS+2H]^{2+}$ and $[SDGRG+2H]^{2+}$ respectively. Under the reported conditions, baseline resolution of both singly and doubly

Table 1 Summary of molecular weight, *m/z*, reduced mobilities and Collision cross section (CCS)

Peptide sequence	MW	Ion	m/z	Experimental Ko (cm^2V^{-1} s^{-1})[a]	Experimental CCS ($Å^2$)[b]
Gly-Arg-Gly-Asp-Ser (GRGDS)	490.5	$[GRGDS+H]^+$	491.5	1.02 ± 0.02	205 ± 2
Gly-Arg-Gly-Asp-Ser (GRGDS)		$[GRGDS+2H]^{2+}$	246.3	1.55 ± 0.05	269 ± 1
Ser-Asp-Gly-Arg-Gly (SDGRG)		$[SDGRG+H]^+$	491.5	1.03 ± 0.02	203 ± 1
Ser-Asp-Gly-Arg-Gly (SDGRG)		$[SDGRG+2H]^{2+}$	246.3	1.52 ± 0.05	274 ± 1
Gly-Arg-Gly-Asp-Thr-Pro (GRGDTP)	601.6	$[GRGDTP+H]^+$	602.6	0.911 ± 0.002	228 ± 2
Gly-Arg-Gly-Asp-Thr-Pro (GRGDTP)		$[GRGDTP+2H]^{2+}$	301.8	1.48 ± 0.05	281 ± 1
Sar-Arg-Gly-Asp-Ser-Pro (SRGDSP)		$[SRGDTP+H]^+$	602.6	0.913 ± 0.002	227 ± 1
Sar-Arg-Gly-Asp-Ser-Pro (SRGDSP)		$[SRGDTP+2H]^{2+}$	301.8	1.49 ± 0.05	278 ± 2
Leu-Arg-Arg-Ala-Ser-Leu-Gly (Kemptide)	771.9	$[Kemptide+H]^+$	772.9	0.749 ± 0.002	276 ± 1
Leu-Arg-Arg-Ala-Ser-Leu-Gly (Kemptide)		$[Kemptide+2H]^{2+}$	387.1	1.31 ± 0.04	314 ± 1
Leu-Arg-Arg-Ala-Ser-Val-Ala (Val^6,Ala^7)Kemptide		$[(Val^6,Ala^7)$ Kemptide$+H]^+$	772.9	0.771 ± 0.002 0.774 ± 0.002	268 ± 2 279 ± 1
Leu-Arg-Arg-Ala-Ser-Val-Ala (Val^6,Ala^7)Kemptide		$[(Val^6,Ala^7)$ Kemptide$+2H]^{2+}$	387.1	1.33 ± 0.04	311 ± 1

The experiments for the different sets of isomeric peptides were performed in triplicates. The listed [a] reduced mobilities and [b] CCS in Table 1 were averaged out and the standard deviation reported as error. The CCS values were calculated from the individual target analyte ions, not the target analyte mixture ions

charged ions of the two isomeric pentapeptide mixture was attainable with PCB-IMS system, illustrating that the resolving power of the present instrument with the 3S-IS setup allows separation for isomeric compounds with smaller differences in CCS values (< 1%). We note that, this is the first time baseline separation has been reported for the singly charged ions of the isomeric reversed sequence pentapeptide mixture using Fourier transformed drift tube IMS with nitrogen as the drift gas.

The primary difference between the two isomeric hexapeptides seen in Fig. 2 is the location of the methyl group. The methyl group on the sarcosine amino group is shifted to the serine thereby converting the sarcosine to glycine and the serine to threonine. Figure 2a and b are the mass selected mobility spectra of isomeric hexapeptides ion mixture obtained with the 3S-IS and 2S-IS respectively. Whereas, Fig. 2c displays the mass selected mobility spectra of individual hexapeptides target analyte ions. According to Table 1, the CCS value of the singly protonated ions were experimentally the same with a difference of 0.4%, significantly smaller than the doubly protonated ion population and remained unseparated. However, a baseline separation was achieved for the doubly protonated ions with the 3S-IS as shown in Fig. 2b. Whereas, with the 2S-IS, a near-to-baseline separation was achieved for the doubly charged ions as seen in Fig. 2a The measurement indicated a difference of 1.0% in the CCS value calculated for the doubly protonated ion. In comparison to the work done by Wu et al.,[22] a difference of 2.3% was recorded for the doubly charged ion species, which resulted in a near-to-baseline separation. This results further demonstrates the improved performance of the 3S-IS to separate ions with significantly smaller differences in their calculated CCS values and also has a higher resolving power than the resolving power of the IMS reported by Wu et al. (RP = 80) [22]. Additionally, the ion counts and resolving power of the hexapeptide ion mixture with the 3S-IS was higher than that of the 2S-IS. For the hexapeptide mixture at *m/z* 602 and *m/z* 301, the recorded ion counts in Table 2 with the 3S-IS were 3.18×10^4 and 5.56×10^4 resulting in a 61.9% and 88.4% increase for *m/z* 602 and *m/z* 301 respectively in comparison to the 2S-IS. For reference, the resolving powers for the hexapeptide mixture with the 3S-IS were 87 and 104 for $[GRGDTP+2H]^{2+}$, $[SRGDSP+2H]^{2+}$ respectively and for the 2S-IS were 80 and 100 for $[GRGDTP+2H]^{2+}$, $[SRGDSP+2H]^{2+}$ respectively. This corresponds to an 8% and 3.8% increase in resolving power for $[GRGDTP+2H]^{2+}$ and $[SRGDSP+2H]^{2+}$ respectively with the 3S-IS in comparison to the 2S-IS. Whereas, the resolving powers recorded for the individual species were 57 for $[GRGDTP+2H]^{2+}$ and 82 for $[SRGDSP+2H]^{2+}$. The calculated CCS values for the doubly protonated ions of SRGDSP and GRGDTP were (278 $Å^2$) and (281 $Å^2$) respectively. Sar**H** + -Arg**H** + −Gly-Asp-Ser-Pro, Gly**H** + -Arg**H** + −Gly-Asp-Thr-Pro are the suggested charge locations for the doubly protonated ions. The closeness of the two charges might presumably cause strong coulombic repulsion. The calculated CCS values suggest that $[GRGDTP+2H]^{2+}$ exhibits a more elongated structure ("stretched out") than $[SRGDSP+2H]^{2+}$. The differences in the gas-phase conformation exhibited by the doubly protonated ions might be due to the differences in gas basicities demonstrated by the N-terminal groups (888.7 kJ/mol for sarcosine and 855.4 kJ/mol for glycine). The conformations of peptides and proteins following electrospraying ionization are impacted by a range of factors

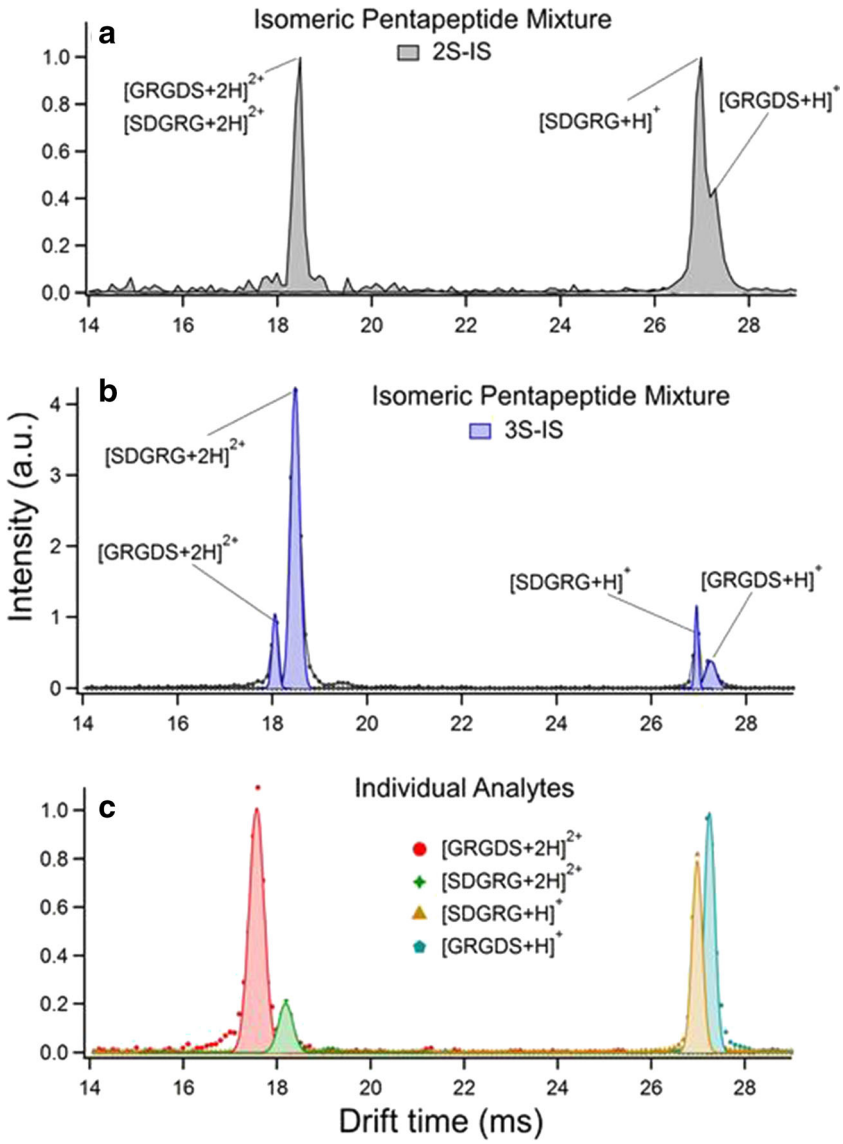

Fig. 1 Mass selected mobility spectra obtained through the FT-IMMS experiment with a frequency sweep from 5 to 10,005 Hz for 8 min using the (**a**) two-state ion shutter (2S-IS) for a mixture of two reversed sequence pentapeptide, (**b**) tri-state ion shutter (3S-IS) for a mixture of two reversed sequence pentapeptide. (**c**) The two pentapeptides were analyzed individually using the 3S-IS

including solvent ionic strength, site(s) of protonation or deprotonation, and gas-phase basicity.[39–42] Regarding the latter property, sarcosine and glycine serve as salient comparisons when considering gas-phase basicity in the context of the present experiments. The differential proton affinity, which is directly related to gas-phase basicity, between the two amino

Table 2 Summary of ion counts for the target analyte ion mixture using the 3S-IS and 2S-IS

Analyte	m/z	Ion counts (3S-IS)	Ion counts (2S-IS)
SDGRG/GRGDS (+1 charge state)	491	$2.25 \times 10^4 \pm 1 \times 10^3$	$3.60 \times 10^3 \pm 4 \times 10^1$
SDGRG/GRGDS (+2 charge state)	246	$9.71 \times 10^3 \pm 4 \times 10^2$	$6.61 \times 10^2 \pm 7 \times 10^1$
GRGDTP/SRGDSP (+1 charge state)	602	$3.18 \times 10^4 \pm 2 \times 10^3$	$1.21 \times 10^4 \pm 4 \times 10^2$
GRGDTP/SRGDSP (+2 charge state)	301	$5.56 \times 10^4 \pm 3 \times 10^3$	$6.47 \times 10^3 \pm 6 \times 10^1$
Kemptide/ (Val^6,Ala^7)-Kemptide (+1 charge state)	772	$6.65 \times 10^4 \pm 5 \times 10^2$	$4.47 \times 10^3 \pm 6 \times 10^1$
Kemptide/ (Val^6,Ala^7)-Kemptide (+2 charge state)	387	$2.22 \times 10^5 \pm 8 \times 10^3$	$4.17 \times 10^4 \pm 1 \times 10^3$

Ion counts recorded in Table 2 were reported from the raw mass spectrum of the FT-IMMS experiments from 5 to 10,005 Hz for 8 min and not the transformed arrival time distribution of the FT-IMMS

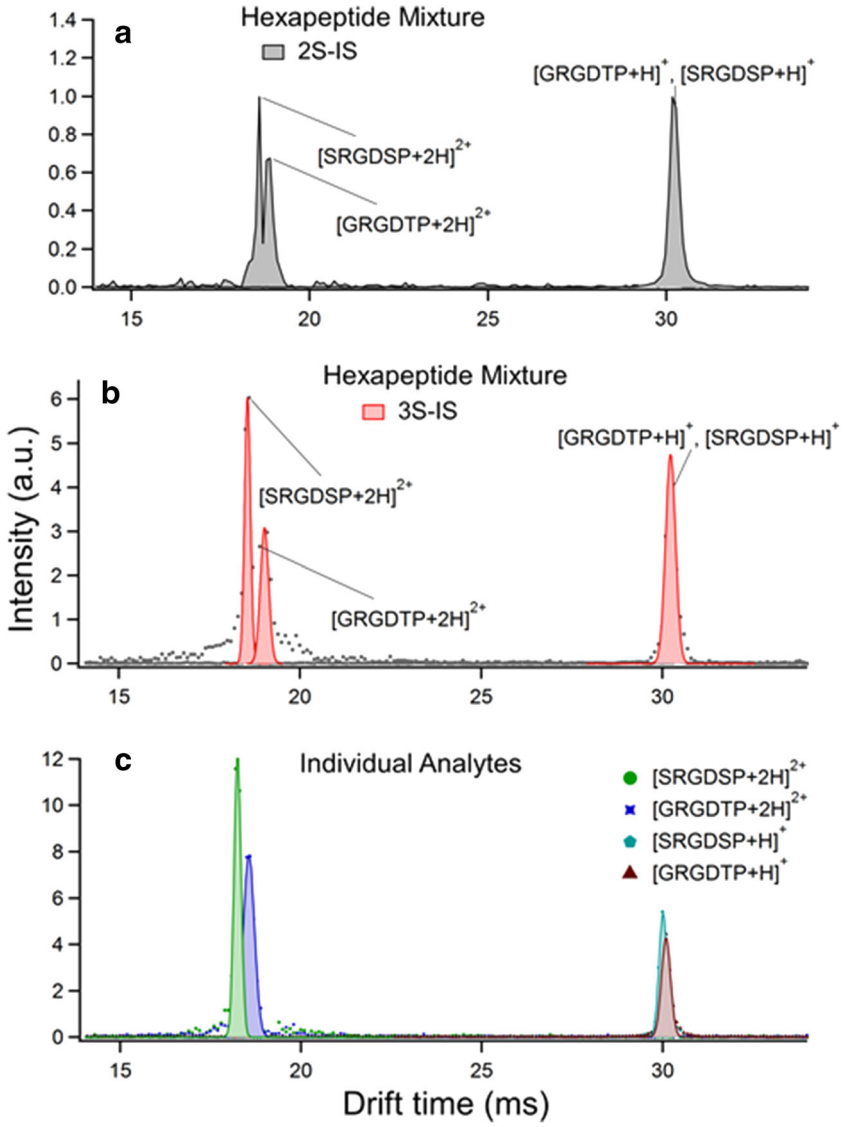

Fig. 2 Mass selected mobility spectra of two isomeric hexapeptide different by the N-terminal amino acids and the fourth amino acid obtained through the FT-IMMS experiment with a frequency sweep from 5 to 10,005 Hz for 8 min using the (**a**) two-state ion shutter (2S-IS) for the ion mixture, (**b**) tri-state ion shutter (3S-IS) for ion mixture. (**c**) The two hexapeptides were individually analyzed using the 3S-IS

acids establishes conditions where different degrees of Coulombic repulsion are present when the sites of protonation are at the two amino acids adjacent to the N-terminus. Under these conditions, in order to accommodate the higher coulombic repulsion between the sarcosine and arginine charge sites, conformational rearrangement is likely in the gas-phase which translates into a different gas-phase ion conformation for Sar**H** + -Arg**H** + −Gly-Asp-Ser-Pro with a CCS lower than that of Gly**H** + -Arg**H** + −Gly-Asp-Thr-Pro. This rationale also extends to the hexapeptide systems where $[GRGDTP+2H]^{2+}$ exhibits a more elongated structure than $[SRGDSP+2H]^{2+}$. Building along this same line, Wu et al.[22] suggested that to overcome the strong Coulombic repulsion, the charge located on the glycine (Gly**H** + -Arg**H** + −Gly-Asp-Thr-Pro) might shift to the carbonyl side on the backbone of the sequence to produce a different gas-phase conformation.[43] The present discussion assumes the charge sites for the doubly charged species are restricted to the N-terminus, however, the possibility of alternative charge configurations cannot be entirely excluded. Figures 1 and 2 display Gaussian fits to the transformed FT-IMMS spectra, however, close examination of the raw traces illustrates that small shoulders exist for some of the doubly charged species. These observations further support the notion that alternative conformations can exist and the core aspects of the discussion regarding Coulombic repulsion hold.

Kemptide and Val^6,Ala^7-kemptide were analyzed and observed as both singly ($[kemptide+H]^+$, $[(Val^6, Ala^7)\text{-}kemptide+H]^+$) and doubly protonated ($[kemptide+2H]^{2+}$, $([Val^6, Ala^7)\text{-}kemptide+2H]^{2+}$) ions as illustrated in Fig. 3. Figure 3 is the mass selected mobility spectra for two heptapeptide ion mixture using 2S-IS (Fig. 3a) and 3S-IS (Fig. 3b). Whereas, Fig. 3c is the mass selected mobility spectra of the individual heptapeptide analyte ions. The difference between the two heptapeptides is the shift of a methyl group

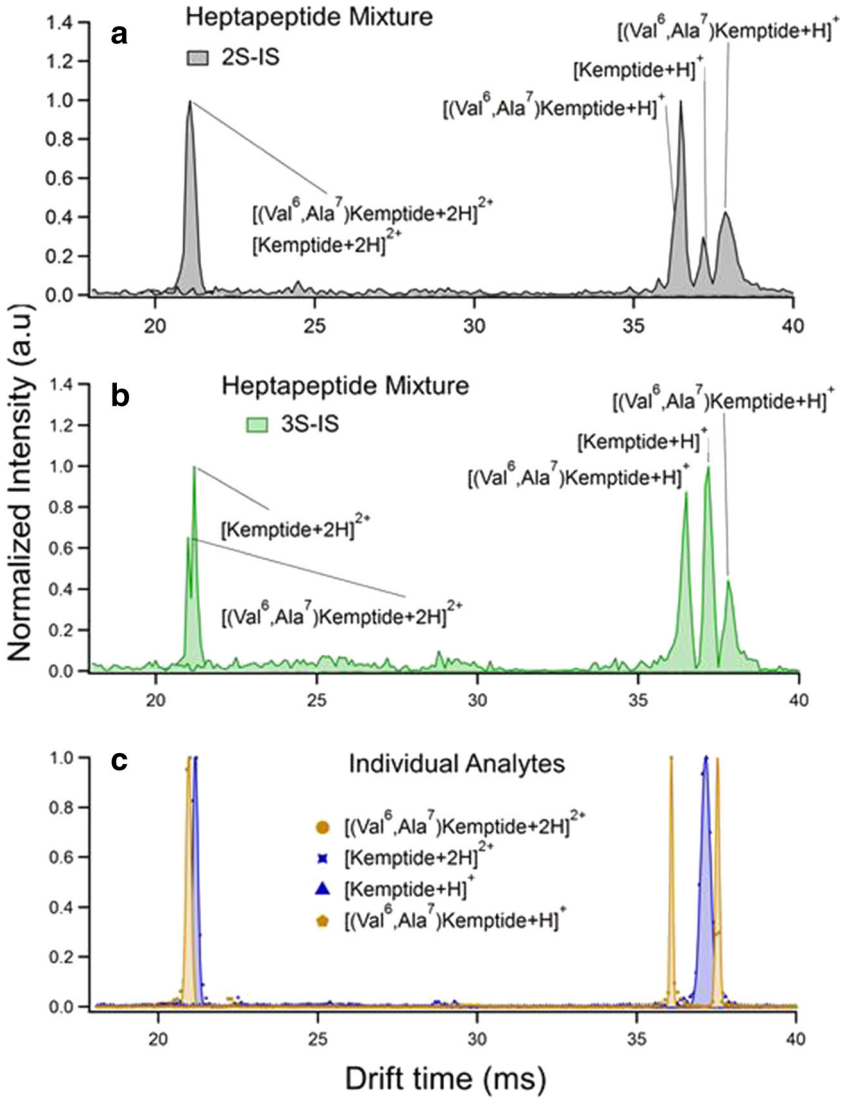

Fig. 3 Mass selected mobility spectra of two isomeric methyl substituted heptapeptides obtained using the FT-IMMS experiment with a frequency sweep from 5 to 10,005 Hz for 8 min using the (**a**) two-state ion shutter (2S-IS) for the ion mixture, (**b**) tri-state ion shutter (3S-IS) for the ion mixture. (**c**) The two hepta-peptides were individually analyzed using the 3S-IS

from the leucine to glycine; converting leucine to valine and glycine to alanine. The possible charge locations for both kemptide and (Val^6, Ala^7)-kemptide singly charged ions are as follows. 1) Leu**H**$^+$-Arg-Arg-Ala-Ser-Leu-Gly / (Val^6, Ala^7), 2) Leu-Arg**H**$^+$-Arg-Ala-Ser-Leu-Gly / (Val^6, Ala^7), 3) Leu-Arg-Arg**H**$^+$-Ala-Ser-Leu-Gly / (Val^6, Ala^7). From Fig. 3a–c, a single ion mobility peak was observed for [kemptide+H]$^+$. If all the proposed charge locations for [kemptide+H]$^+$ had been produced during the electrospray process then three ion populations would be present in the system. While baseline separation of these protomers may not be possible using the present system, a modicum of peak broadening would be expected under such conditions. Instead, a single ion mobility peak was observed for [kemptide+H]$^+$. However, for [(Val^6, Ala^7)-kemptide+H]$^+$, two ion mobility peaks were observed in Fig. 3a–c. The two ion mobility peaks for the Val^6, Ala^7-kemptide singly charged ion demonstrates that two of the listed proposed charge location configurations were captured in the gas-phase when Val^6, Ala^7-kemptide was electrosprayed. The CCS values calculated from the individual target analyte ions for the singly charged ions were 276 Å^2 for kemptide and 268 Å^2, 279 Å^2 for Val^6, Ala^7-kemptide as observed in Table 1. These CCS values correspond to differences of 3.0% and 1.1% which resulted in the baseline separation as shown in Fig. 3a and b using the 2S-IS and 3S-IS respectively. For the doubly protonated species, the suggested charge locations are as follows. 1) Leu**H**$^+$-Arg**H**$^+$-Arg-Ala-Ser-Leu-Gly / (Val^6, Ala^7), 2) Leu**H**$^+$-Arg-Arg**H**$^+$-Ala-Ser-Leu-Gly / (Val^6, Ala^7), 3) Leu-Arg**H**$^+$-Arg**H**$^+$-Ala-Ser-Leu-Gly / (Val^6, Ala^7). As seen in Fig. 3, a single ion mobility peak was observed for both [kemptide+2H]$^{2+}$ and [(Val^6, Ala^7)-kemptide+2H]$^{2+}$. The calculated CCS values from the individual heptapeptide target analyte ions were 314 Å^2 for [kemptide+2H]$^{2+}$ and 311 for [(Val^6, Ala^7)-kemptide+2H]$^{2+}$ as reported in Table 1. These CCS values correspond to a difference of 0.98% and partial resolution in the mobility

domain with the 3S-IS as shown in Fig. 3b. However, for the 2S-IS, the doubly protonated ions ([kemptide+2H]$^{2+}$, [(Val^6, Ala^7)-kemptide+2H]$^{2+}$) of the heptapeptide mixture were overlapped and hence remained unresolved in the mobility domain as demonstrated in Fig. 3a. We note that in comparison to the work done by Wu et al.,[22] the calculated CCS values for the doubly protonated ions showed a small difference of about 0.5% and hence no separation was achieved for the doubly charged ions ([kemptide+2H]$^{2+}$, ([Val^6, Ala^7)-kemptide+2H]$^{2+}$). For reference, the resolving powers for this mixture using the 3S-IS were 124 for [kemptide+H]$^+$ and 117, 102 for [(Val^6, Ala^7)-kemptide+H]$^+$ (corresponding to the first and last peak at m/z 772 in Fig. 3, starting from the left). For the 2S-IS, the resolving power for [kemptide+2H]$^{2+}$ was 100 and 90, 60 for [(Val^6, Ala^7)-kemptide+H]$^+$ (corresponding to the first and last peak at m/z 772 in Fig. 3, starting from the left). Whereas, the resolving powers for the individual species were 106 for [kemptide+H]$^+$ and 98, 95 for [(Val^6, Ala^7)-kemptide+H]$^+$. Overall, an increase in ion counts and slight increase in resolving powers was achieved with the 3S-IS in comparison to the 2S-IS for the heptapeptide ion mixture. Although baseline resolution of the doubly protonated ions of the heptapeptide analyte mixture was not achieved using the 3S-IS, clear distinction of the two heptapeptide analyte ions is observed in comparison to the 2S-IS, where the doubly charged ions of the heptapeptide mixture were completely overlapped. Raw signal traces for *m/z* 386 from the FT-IMMS experiments are shown in Fig. 4 for kemptide/ (Val^6, Ala^7)-kemptide ion mixture using the 3S-IS and 2S-IS. From Fig. 4, a continuous increase in ion signal is observed for the 3S-IS throughout the duration of the experiment. Whereas, in the case of the 2S-IS, the ion intensity remains somewhat

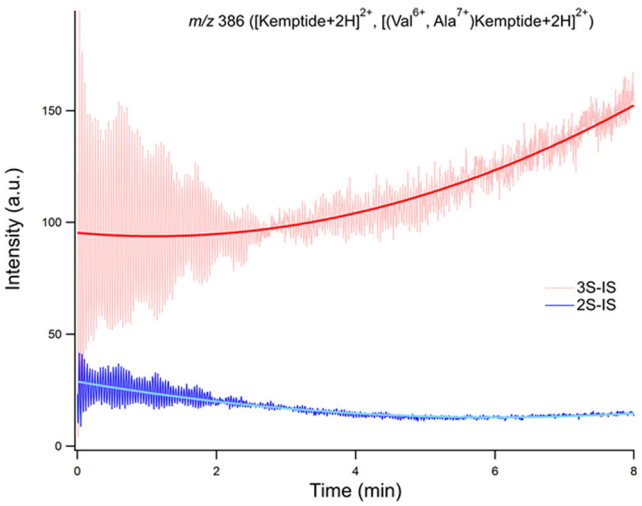

Fig. 4 Raw signal traces for m/z 386 from the FT-IMMS experiments are shown for kemptide/(Val^6,Ala^7)-kemptide mixture using the 3S-IS and 2S-IS. The raw signal traces for the ion populations using 3S-IS clearly exhibit two different ion populations. A polynomial xoffset fit is fitted to each signal trace just for the purpose of demonstrating the rise in ion signal

constant throughout the course of the experiment. This observation trends with our prior publication, where a comparison plot of the raw signal traces was made for the TXA, T5 ion using the 3S-IS and 2S-IS.[21] Fig. 4 and the data reported in Table 2, additionally highlight the increase in ion counts gained for the target analyte ion mixture using the 3S-IS in comparison to the 2S-IS.

Conclusion

Using an atmospheric, dual gate drift tube ion mobility coupled to a linear ion trap mass spectrometer using linear frequency modulation and the Fourier transform to recover gas-phase ion mobilities, we compare the separating capacity of system using the 3S-IS and 2S-IS principles for three pairs of peptide mixtures. From the results of the mobility separations, we illustrate the ability of multiplexing systems coupled with 3S-IS to enhance mobility separations and ion current. For each set of the isomeric peptides, both single and double protonated ions were observed in the mobility domain. For the three pairs peptide mixtures analyzed, the ion counts recorded for the singly and doubly protonated ions were higher with the 3S-IS compared to the 2S-IS. Similarly, the resolving powers for the target analyte ions were slightly higher (21%) with the 3S-IS in comparison to the 2S-IS. Compared to previous efforts of separating the same sets of isomeric peptides using drift tube IMMS with a Bradbury-Nelson ion shutter, the present work focuses on the benefits of using tri-state ion shutter (3S-IS) in FT-based IMMS experiments for complex analytical separation such as isomeric species. Separations achieved for isomeric peptides with the same *m/z* and charge state were due to small differences in their gas-phase structural conformation measurable as ion-neutral collision cross section (CCS). Under the outlined conditions, the resolving power of the instrument with the 3S-IS configuration used in this study allows separation of isomeric compounds with less than 1% differences in their CCS values.

Acknowledgments Support for P.K.B. was provided by Army Research Office (Award# W911NF1510619).

References

1. Syka JEP, Coon JJ, Schroeder MJ, Shabanowitz J, Hunt DF (2004) Peptide and protein sequence analysis by electron transfer dissociation mass spectrometry. Proc Natl Acad Sci U S A 101(26):9528–9533
2. O.N. Jensen, E. Sachon: Protein and peptide analysis by matrix-assisted laser desorption/ionization tandem mass spectrometry (MALDI MS/MS), 10.1201/9781420017090.ch5,(2007)
3. Link AJ, Eng J, Schieltz DM, Carmack E, Mize GJ, Morris DR, Garvik BM, Yates JR 3rd (1999) Direct analysis of protein complexes using mass spectrometry. Nat Biotechnol 17(7):676–682

4. Lewis JK, Wei J, Siuzdak G (2006) Matrix-assisted laser desorption/ionization mass spectrometry in peptide and protein analysis. Encyclopedia of Analytical Chemistry, Applications, Theory and Instrumentation
5. Coon JJ, Syka JEP, Shabanowitz J, Hunt DF (2005) Tandem Mass Spectrometry for Peptide and Protein Sequence Analysis 38(4): 519–523. https://doi.org/10.2144/05384te01
6. Giesemann, A-J. Jaeger, H, Norman, A.L., Krouse, H.R., Brand, W.A.: Online Sulfur-Isotope Determination Using an Elemental Analyzer Coupled to a Mass Spectrometer, https://doi.org/10.1021/ac00090a005, (1994), 66, 18, 2816, 2819
7. C.A. Johnson, C.A. Stricker, C.A. Gulbransen, M.P. Emmons: Determination of δ13C, δ15N, or δ34S by isotope-ratio-monitoring mass spectrometry using an elemental analyzer, 10.3133/tm5d4, (2018)
8. Gandhi, H., Wiegner, T.N., Ostrom, P.H., Kaplan, L.A., Ostrom, N.E.: Isotopic(13C) analysis of dissolved organic carbon in stream water using an elemental analyzer coupled to a stable isotope ratio mass spectrometer, https://doi.org/10.1002/rcm.1426, (2004), 18, 8, 903, 906
9. Lane AN, Fan TW-M, Xie Z, Moseley HNB, Higashi RM (2009) Isotopomer analysis of lipid biosynthesis by high resolution mass spectrometry and NMR. Anal Chim Acta 651(2):201–208
10. J.A. Vogt, K. Schroer, K. Hölzer, C. Hunzinger, M. Klemm, K. Biefang-Arndt, S. Schillo, M.A. Cahill, A. Schrattenholz, H. Matthies, W Stegmann.: Protein abundance quantification in embryonic stem cells using incomplete metabolic labelling with ^{15}N amino acids, matrix-assisted laser desorption/ionisation time-of-flight mass spectrometry, and analysis of relative isotopologue abundances of peptides, 10.1002/rcm.1045, (2003), 17, 12, 1273, 1282
11. Young ED, Rumble D, Freedman P, Mills M (2016) A large-radius high-mass-resolution multiple-collector isotope ratio mass spectrometer for analysis of rare isotopologues of O2, N2, CH4 and other gases. Int J Mass Spectrom 401:1–10
12. Tao WA, Gozzo FC, Cooks RG (2001) Mass spectrometric quantitation of chiral drugs by the kinetic method. Anal Chem 73(8): 1692–1698
13. Wu L, Meurer EC, Young B, Yang P, Eberlin MN, Cooks RG (2004) Isomeric differentiation and quantification of α, β-amino acid-containing tripeptides by the kinetic method: alkali metal-bound dimeric cluster ions. Int J Mass Spectrom 231(2-3):103–111
14. J.S. Splitter, F. Tureček: Applications of mass spectrometry to organic stereochemistry. (1994)
15. von Helden G, von Helden G, Wyttenbach T, Bowers MT (1995) Conformation of Macromolecules in the Gas Phase: Use of Matrix-Assisted Laser Desorption Methods in Ion Chromatography 267(5203):1483–1485. https://doi.org/10.1126/science.267.5203.1483
16. Ruotolo BT, Robinson CV (2006) Aspects of native proteins are retained in vacuum. Curr Opin Chem Biol 10(5):402–408
17. Benesch JLP, Ruotolo BT, Simmons DA, Robinson CV (2007) Protein complexes in the gas phase: technology for structural genomics and proteomics. Chem Rev 107(8):3544–3567
18. Dear GJ, Munoz-Muriedas J, Beaumont C, Roberts A, Kirk J, Williams JP, Campuzano I (2010) Sites of metabolic substitution: investigating metabolite structures utilising ion mobility and molecular modelling. Rapid Commun Mass Spectrom 24(21):3157–3162
19. Ruotolo BT, Benesch JLP, Sandercock AM, Hyung S-J, Robinson CV (2008) Ion mobility–mass spectrometry analysis of large protein complexes. Nat Protoc 3(7):1139–1152
20. Giles K, Williams JP, Campuzano I (2011) Enhancements in travelling wave ion mobility resolution. Rapid Commun Mass Spectrom 25(11):1559–1566
21. Kwantwi-Barima P, Reinecke T, Clowers BH (2019) Increased ion throughput using tristate ion-gate multiplexing. Analyst. 144(22): 6660–6670
22. Wu C, Siems WF, Klasmeier J, Hill HH Jr (2000) Separation of isomeric peptides using electrospray ionization/high-resolution ion mobility spectrometry. Anal Chem 72(2):391–395
23. Stow SM, Causon TJ, Zheng X, Kurulugama RT, Mairinger T, May JC, Rennie EE, Baker ES, Smith RD, McLean JA, Hann S, Fjeldsted JC (2017) An Interlaboratory evaluation of drift tube ion mobility–mass spectrometry collision cross section measurements. Anal Chem 89(17):9048–9055
24. May JC, Goodwin CR, Lareau NM, Leaptrot KL, Morris CB, Kurulugama RT, Mordehai A, Klein C, Barry W, Darland E (2014) Others: conformational ordering of biomolecules in the gas phase: nitrogen collision cross sections measured on a prototype high resolution drift tube ion mobility-mass spectrometer. Anal Chem 86(4):2107–2116
25. Clowers BH, Siems WF, Yu Z, Davis AL (2015) A two-phase approach to Fourier transform ion mobility time-of-flight mass spectrometry. Analyst. 140(20):6862–6870
26. Reinecke T, Naylor CN, Clowers BH (2019) Ion multiplexing: maximizing throughput and signal to noise ratio for ion mobility spectrometry. Trends Analyt Chem 116:340–345
27. Clowers BH, Siems WF, Hill HH, Massick SM (2006) Hadamard transform ion mobility spectrometry. Anal Chem 78(1):44–51
28. Morrison KA, Siems WF, Clowers BH (2016) Augmenting ion trap mass spectrometers using a frequency modulated drift tube ion mobility spectrometer. Anal Chem 88(6):3121–3129
29. Morrison KA, Bendiak BK, Clowers BH (2016) Enhanced mixture separations of metal adducted tetrasaccharides using frequency encoded ion mobility separations and tandem mass spectrometry. J Am Soc Mass Spectrom 28:664–677
30. Poltash ML, McCabe JW, Shirzadeh M, Laganowsky A, Clowers BH, Russell DH (2018) Fourier transform-ion mobility-Orbitrap mass spectrometer: a next-generation instrument for native mass spectrometry. Anal Chem 90(17):10472–10478
31. Knorr FJ, Eatherton RL, Siems WF, Hill HH Jr (1985) Fourier transform ion mobility spectrometry. Anal Chem 57(2):402–406
32. Reinecke T, Davis AL, Clowers BH (2019) Determination of gas-phase ion mobility coefficients using voltage sweep multiplexing. J Am Soc Mass Spectrom 30(6):977–986
33. Ibrahim YM, Garimella SVB, Tolmachev AV, Baker ES, Smith RD (2014) Improving ion mobility measurement sensitivity by utilizing helium in an ion funnel trap. Anal Chem 86(11):5295–5299
34. Kirk AT, Grube D, Kobelt T, Wendt C, Zimmermann S (2018) High-resolution high kinetic energy ion mobility spectrometer based on a low-discrimination tristate ion shutter. Anal Chem 90(9):5603–5611
35. Langejuergen J, Allers M, Oermann J, Kirk A, Zimmermann S (2014) High kinetic energy ion mobility spectrometer: quantitative analysis of gas mixtures with ion mobility spectrometry. Anal Chem 86(14):7023–7032
36. Reinecke T, Clowers BH (2018) Implementation of a flexible, open-source platform for ion mobility spectrometry. HardwareX. 4:e00030
37. Garcia L, Saba C, Manocchio G, Anderson GA, Davis E, Clowers BH (2017) An open source ion gate pulser for ion mobility spectrometry. Int J Ion Mobil Spectrom 20(3-4):87–93
38. Bush MF, Hall Z, Giles K, Hoyes J, Robinson CV, Ruotolo BT (2010) Collision cross sections of proteins and their complexes: a calibration framework and database for gas-phase structural biology. Anal Chem 82(22):9557–9565
39. Jhingree JR, Bellina B, Pacholarz KJ, Barran PE (2017) Charge mediated compaction and rearrangement of gas-phase proteins: a case study considering two proteins at opposing ends of the

structure-disorder continuum. J Am Soc Mass Spectrom 28(7): 1450–1461
40. Ehrmann BM, Henriksen T, Cech NB (2011) Relative importance of basicity in the gas phase and in solution for determining selectivity in electrospray ionization mass spectrometry. J Am Soc Mass Spectrom 19:719–728
41. Schnier PD, Gross DS, Williams ER (1995) Electrostatic forces and dielectric polarizability of multiply protonated gas-phase cytochrome c ions probed by ion/molecule chemistry. J Am Chem Soc 117(25):6747–6757
42. Mirza UA, Chait BT (1994) Effects of Anions on the Positive Ion Electrospray Ionization Mass Spectra of Peptides and Proteins 66(18):2898–2904. https://doi.org/10.1021/ac00090a017
43. J. Wu, C.B. Lebrilla: Gas-phase basicities and sites of protonation of glycine oligomers (Glyn; n = 1–5), 10.1021/ja00061a027, (1993), 115, 8, 3270, 3275